Title

Coupling stable isotopes and water chemistry to assess the role of hydrological and biogeochemical processes on riverine nitrogen sources

Authors

Hu, Minpeng
Liu, Yanmei
Zhang, Yufu
et al.

Publication Date

2019-03-01

DOI

10.1016/j.watres.2018.11.082

Peer reviewed

Water Research 150 (2019) 418–430

Contents lists available at ScienceDirect

Water Research

journal homepage: www.elsevier.com/locate/watres

Coupling stable isotopes and water chemistry to assess the role of hydrological and biogeochemical processes on riverine nitrogen sources

Minpeng Hu [a, b], Yanmei Liu [a], Yufu Zhang [a], Randy A. Dahlgren [d], Dingjiang Chen [a, c, *]

[a] College of Environmental & Resource Sciences, Zhejiang University, Hangzhou, 310058, China
[b] Zhejiang Provincial Key Laboratory of Subtropical Soil and Plant Nutrition, Zhejiang University, Hangzhou, 310058, China
[c] Ministry of Education Key Laboratory of Environment Remediation and Ecological Health, Zhejiang University, Hangzhou, 310058, China
[d] Department of Land, Air, and Water Resources, University of California, Davis, CA, 95616, USA

ARTICLE INFO

Article history:
Received 12 July 2018
Received in revised form
15 November 2018
Accepted 29 November 2018
Available online 6 December 2018

Keywords:
Nitrogen dynamics
Dual stable isotopes
Source identification
Legacy effect

ABSTRACT

Accurate source identification is critical for optimizing water pollution control strategies. Although the dual stable isotope ($^{15}N\text{-}NO_3^-/^{18}O\text{-}NO_3^-$) approach has been widely applied for differentiating riverine nitrogen (N) sources, the relatively short-term (<1 yr) $^{15}N\text{-}NO_3^-/^{18}O\text{-}NO_3^-$ records typically used in previous studies often hinders rigorous assessment due to high temporal variability associated with watershed N dynamics. Estimated contributions of legacy N sources in soils and groundwater to riverine N export by modeling approaches in many previous studies also lack validation from complementary information, such as multiple stable isotopes. This study integrated three years of multiple stable isotope ($^{15}N\text{-}NO_3^-/^{18}O\text{-}NO_3^-$ and $^{2}H\text{-}H_2O/^{18}O\text{-}H_2O$) and hydrochemistry measurements for river water, groundwater and rainfall to elucidate N dynamics and sources in the Yongan watershed (2474 km^2) of eastern China. Nonpoint source N pollution dominated and displayed considerable seasonal and spatial variability in N forms and concentrations. Information from $\delta^{15}N\text{-}NO_3^-$ and $\delta^{18}O\text{-}NO_3^-$ indicated that riverine N dynamics were regulated by contributing sources, nitrification and denitrification, as well as hydrological processes. For the three examined catchments and entire watershed, slow subsurface and groundwater flows accounted for >75% of river discharge and were likely the major hydrological pathways for N delivery to the river. Riverine NO_3^- sources varied with dominant land use ($p < 0.001$), with the highest contributions of groundwater (60%), wastewater (35%), and soil (50%) occurring in agricultural, residential and forest catchments, respectively. For the entire watershed, groundwater (~50%) and soil N (>30%) were the dominant riverine NO_3^- sources, implying considerable potential for N pollution legacy effects. Results were consistent with observed nitrous oxide dynamics and N sources identified in previous modeling studies. As the first attempt to apply multiple isotope tracers for exploring and quantifying N transformation and transport pathways, this study provides an integrated approach for verifying and understanding the N pollution legacy effects observed in many watersheds worldwide. This study highlights that river N pollution control in many watersheds requires particular attention to groundwater restoration and soil N management in addition to N input control strategies.

1. Introduction

Increasing anthropogenic nitrogen (N) inputs have resulted in water quality impairments, degradation of aquatic ecosystem health, eutrophication and hypoxia in aquatic ecosystems worldwide (Galloway et al., 2004). Accurate identification and quantification of riverine N sources are critical for optimizing pollution control strategies at the watershed scale. Various lumped watershed models (e.g., export coefficient models, SPARROW, and PolFlow) and mechanistic models (e.g., AGNPS, HSPF, and SWAT) are available for estimating riverine N sources (Borah and Bera, 2004; Wellen et al., 2015). However, riverine N source apportionment remains a challenge, especially because of insufficient data. For

* Corresponding author. College of Environmental & Resource Sciences, Zhejiang University, Hangzhou, 310058, Zhejiang Province, China.
E-mail address: chendj@zju.edu.cn (D. Chen).

https://doi.org/10.1016/j.watres.2018.11.082
0043-1354/

example, mechanistic models typically require large amounts of data for calibration and validation, resulting in difficulties for application in many watersheds (Borah and Bera, 2004; Chen et al., 2014b). Lumped models, which usually provide a simplified understanding of N sources and transfer dynamics from the watershed to rivers, also require information on many watershed attributes, as well as N discharge from sewage treatment facilities and industries. In practice, current models are usually calibrated to measured river discharge and N loads at the watershed outlet, hindering assessment of how realistic these models simulate hydrological and biogeochemical processes throughout various subcatchments within a watershed (Wellen et al., 2015). Thus, watershed-scale simulation modeling has many challenges for practical application, especially for elucidating and validating specific sources and processes.

The dual nitrate stable isotope ($^{15}N\text{-}NO_3^-/^{18}O\text{-}NO_3^-$) approach provides an efficient alternative/complementary tool for differentiating riverine N sources, since each N source often has an unique isotopic signature (Kendall et al., 2007; Xue et al., 2009). Transformation processes (e.g., nitrification and denitrification) associated with N delivery from sources to receiving waters are also recorded by nitrate (NO_3^-) isotopic composition (Kendall et al., 2007; Xue et al., 2009; Xia et al., 2017). The dual NO_3^- stable isotope approach (usually coupled with Bayesian statistics, Parnell et al., 2010) has been successfully applied to assess N transformation processes and sources (e.g., atmospheric deposition, soil pools, chemical fertilizers, manure/sewage) in surface waters and groundwater. For example, the denitrification process in groundwater (Xue et al., 2009; Ji et al., 2017; Minet et al., 2017) and river water (Kaushal et al., 2011; Xia et al., 2017; Yi et al., 2017) was quantified using dual NO_3^- stable isotope data. Furthermore, the dual stable isotope approach was applied to quantify the major contributors of riverine NO_3^- in forest (Ohte, 2013), agricultural, sub-urban (Yang et al., 2013; Ji et al., 2017; Xia et al., 2017) and urban (Yang and Toor, 2016) catchments. In the majority of these studies, dual isotope records were collected for a short-term period (<1 yr), which hinders rigorous assessment of watershed N dynamics and sources given the large temporal variability in watershed processes (Yi et al., 2017; Yang et al., 2013). Additionally, few studies have attempted to verify dual NO_3^- stable isotope results by comparing to hydrological and biogeochemical information from other isotopes and hydrochemistry (Xue et al., 2009; Abbott et al., 2016; Minet et al., 2017; Yi et al., 2017).

Increasing evidence indicates that N leaching from legacy sources in soils and groundwater is a major cause for increasing riverine N exports despite significant declines in anthropogenic N inputs (Meals et al., 2010; Hamilton, 2012; Van Meter et al., 2017; Chen et al., 2018). Such legacy effects are related to the lag time (ranging from months to decades) elapsed between watershed N inputs and riverine export as regulated by hydrological and biogeochemical processes (Howden et al., 2011; Chen et al., 2018; Van Meter et al., 2018). However, the legacy effect is not rigorously addressed and formulated in most current watershed models (e.g., SWAT, HSPF, and AGNPS) due to limited knowledge concerning hydrological and biogeochemical mechanisms affecting the fate and transport of N while passing through soil, vadose zone, and groundwater to the river network (Meals et al., 2010; Covino, 2017; Moatar et al., 2017; Chen et al., 2018; Thomas and Abbott, 2018). Groundwater/baseflow N contributions to riverine N export have been estimated by combining hydrological models and water chemistry monitoring data or regression models for estimating riverine N loads (Table 1). However, these estimates are subject to uncertainties associated with use of empirical relationships in hydrological models (He and Lu, 2016) and lack of validation from complementary information, such as multiple stable isotopes. Quantitative information concerning legacy N contributions from soils and groundwater to riverine N loads is critical for optimizing pollution control strategies (Sanford and Pope, 2013; Bouraoui and Grizzetti, 2014). Furthermore, isotope signals for legacy N in soils and groundwater are mixed and overlapping due to different N sources and cycling processes over time. This could introduce considerable uncertainty in apportioning riverine N to conventional sources (e.g., atmospheric deposition, soils, chemical fertilizers, and manure/sewage) by the dual stable isotope approach alone.

To overcome limitations associated with previous applications of the dual stable isotope approach, as well as previous estimates of legacy N contributions, this study addressed watershed N sources and cycling over a 3-year period using monthly records of multiple isotopes ($^{15}N\text{-}NO_3^-/^{18}O\text{-}NO_3^-$ and $^{2}H\text{-}H_2O/^{18}O\text{-}H_2O$) and hydrochemistry for river water, groundwater and rainfall at multiple sites in the Yongan River watershed of eastern China. Major objectives of this integrated analysis were to (1) reveal spatial and seasonal variations of riverine N dynamics; (2) assess roles of hydrological and biogeochemical processes on riverine N dynamics; and (3) apportion riverine N to soil, groundwater and wastewater sources. Results of this study provide a level of verification for previous studies examining legacy N contributions in the Yongan watershed, as well as improve our quantitative understanding of N dynamics and the N-leaching lag effect at the watershed scale. As the first attempt to apply multiple isotope tracers for exploring and quantifying N transformation and transport pathways, this study provides an integrated approach for verifying and understanding N pollution legacy effects observed in many watersheds worldwide.

2. Material and methods

2.1. Study area

The Yongan River watershed is a typical rainfall-dominated watershed with predominantly forest and agricultural land use in eastern Zhejiang Province, China (Fig. 1). The river drains 2474 km^2 and has an average discharge of 72.9 $m^3\ s^{-1}$ at the downstream outlet sampling site (Fig. 1). Climate is subtropical monsoon with an average annual temperature and precipitation of 17.4 °C and 1400 mm, respectively. Rainfall mainly occurs in May–October (~67%) with a typhoon season in July–September. Agricultural land (including paddy field, garden plot and dryland) averaged ~12% of total watershed area in recent decades, with developed lands, forest, and barren lands contributing ~3, ~67, and ~18%, respectively (Table 2). Red (Oxisols), yellow (Ultisols), and lithological (Entisols) soil groups are the dominant soil types and accounted for 64.6, 15.4, and 1.5% of total soil area, respectively (Chen et al., 2014a). Daily water discharge for the downstream outlet site and daily precipitation and temperature (2014–2017) for the watershed were obtained from the local Hydrology Bureau and Weather Bureau, respectively. Land-use distribution and elevation were obtained from the local Land Resource Bureau by extracting from remote sensing images and digital elevation models and subsequent verification by field investigation. Additional information on Yongan watershed climate, hydrology and river networks can be found in Section 1 of Supporting Information (SI).

2.2. Field sampling

Water samples were collected on a monthly basis during 2014–2017 (Fig. 2) from upstream to downstream, including 12 sampling sites (4 mainstem sites, 5 major tributaries, and 3 groundwater sites) (Fig. 1). Surface water samples were collected at 3–5 points across the river channel and composited to obtain a

Table 1
Baseflow contributions of water and nitrogen to riverine export in reported references.

Study region	Water contribution (%)	N contribution (%)	Methods	Reference
Lake Michigan, USA	63	38	Hydrograph separation approaches (e.g., HYSEP1, HYSEP2, HYSEP3, UKIH, PART, BFLOW) for baseflow separation; Two-dimensional, finite-element, transport model SUTRA for N load estimation	Cherkauer et al. (1992)
MCR watershed, north of Harrisburg, USA	56	56	Water chemistry monitoring during baseflow conditions and storm events	Pionke et al. (1996)
A monitoring station site in Daejeon, Korea	61	60	Hydrograph separation program (PULSE) combined with water chemistry monitoring	Kim et al. (2010)
The Shaying river basin, China	39	40	Groundwater flow model (MODFLOW) combined with a numerical simulation software (MT3DMS)	Chen (2013)
Seven USGS sites in wide range of BFI values, USA	12–84	19–97	The "BFI Program" combined with LOADEST model	Tesoriero et al. (2013)
The Yongan River watershed, southeastern China	82	67	The revised Regional Nutrient Management model was used to estimate groundwater and N contribution	Hu et al. (2018)
Subwatershed of Mahantango Creek, Susquehanna River, USA	64	65	Hydrograph separation methods based on recession analysis combined with the FLUXMASTER and LOADEST model	Zhu et al. (2011)
Two rice agriculture catchment, subtropical central China	28–42	27–37	HYSEP and recursive digital filter methods combined with the ESTIMATOR program	Wang et al. (2015)
Raccoon River watershed, west central Iowa, USA	54	67	HYSEP and recursive digital filter methods combined with the ESTIMATOR	Schilling and Zhang (2004)
Sub-watersheds of the Capitol Region Watershed, Minnesota, USA	27–66	31–68	Baseflow separated from comparison by hydrographs to baseflow rates during known dry periods combined with water chemistry monitoring	Janke et al. (2014)
The Yongan River watershed, southeastern China	79	76	Stable isotopes of water (^{2}H-H_2O/^{18}O-H_2O) combined with N stable isotopes (^{15}N-NO_3^-/^{18}O-NO_3^-)	**This study**

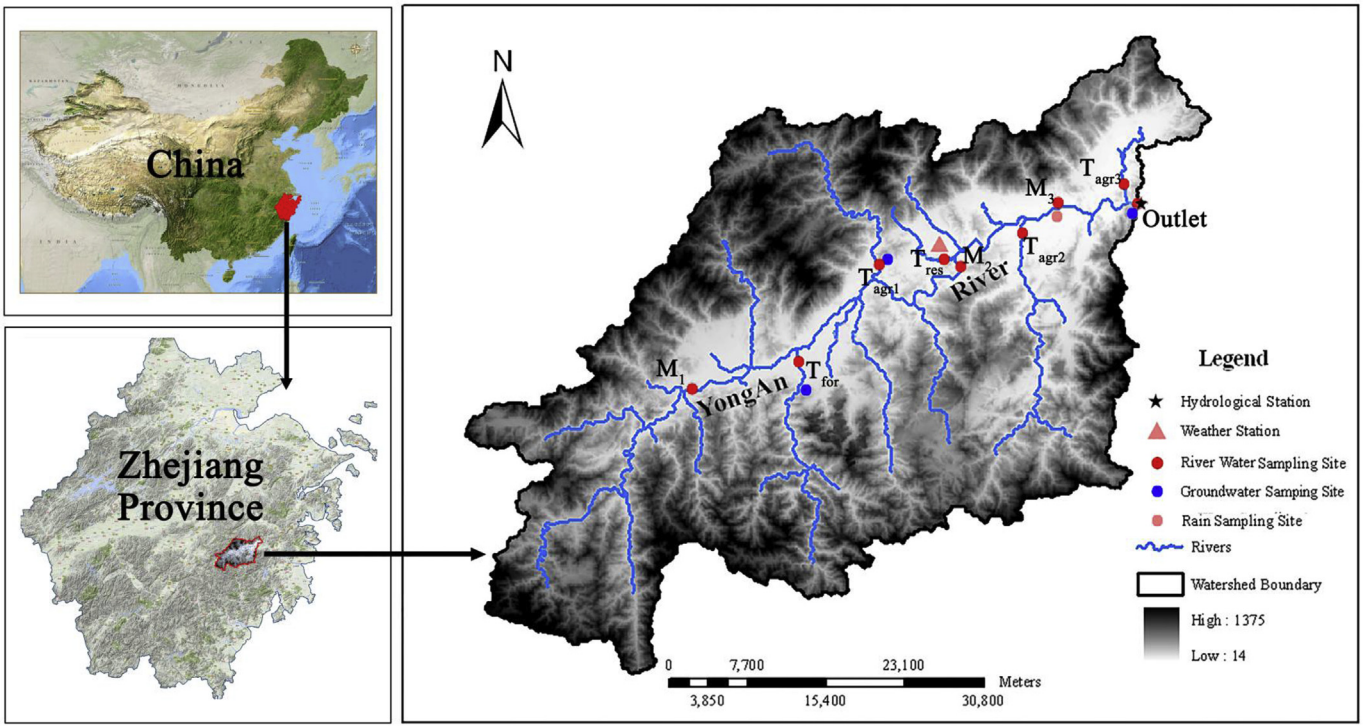

Fig. 1. Location of the Yongan watershed in China and Zhejiang Province and the sampling sites for river water, groundwater and rainfall. "M" represents mainstem, "T" represents tributary. Subscript "agr" represents agricultural tributary, "for" represents forest tributary and "res" represents residential tributary.

single depth-width integrated sample. The Weather Bureau collected and preserved (filtered + refrigeration) rainfall samples on an event basis to provide a monthly composite sample. The composite rainfall sample was a volume-weighted mixture of all rainfall events and was used for water chemistry and stable isotope analysis. Three wells were established in the agricultural tributary (GW_{agr}, 6 m depth), forest tributary (GW_{for}, 6 m depth), and at the watershed outlet (GW_{outlet}, 15 m depth) (Fig. 1). Wells were located 100–200 m from the river channel and screened at depths of 3–6 m for GW_{agr} and GW_{for} and at depths of 5–8 m for GW_{outlet}. Groundwater samples were collected using a peristatic pump to purge a minimum of 3 well volumes of water before collecting a representative sample for water quality analysis. All water samples were immediately sealed and stored at 4 °C.

Table 2
Land-use distribution for sub-catchments and the entire Yongan watershed.

Catchments	Drainage area (km^2)	A (%)	D (%)	F (%)	N (%)	PF (%)	PD	AD
$Trib_{agr2}$	357	11	2	74	23	6%	226	88
$Trib_{agr3}$	163	44	1	54	1	20	287	55
$Trib_{agr1}$	202	14	1	71	14	6	274	110
$Trib_{res}$	35	21	9	49	21	10	828	136
$Trib_{for}$	218	3	1	76	20	2	79	35
Entire watershed	2474	13	3	67	17	6	288	99

A - agricultural lands, D - developed lands, F - forest lands, N - non-utilized lands, PF → paddy field, PD → population density (capita km^{-2}); AD → domestic animal density (capita km^{-2}).

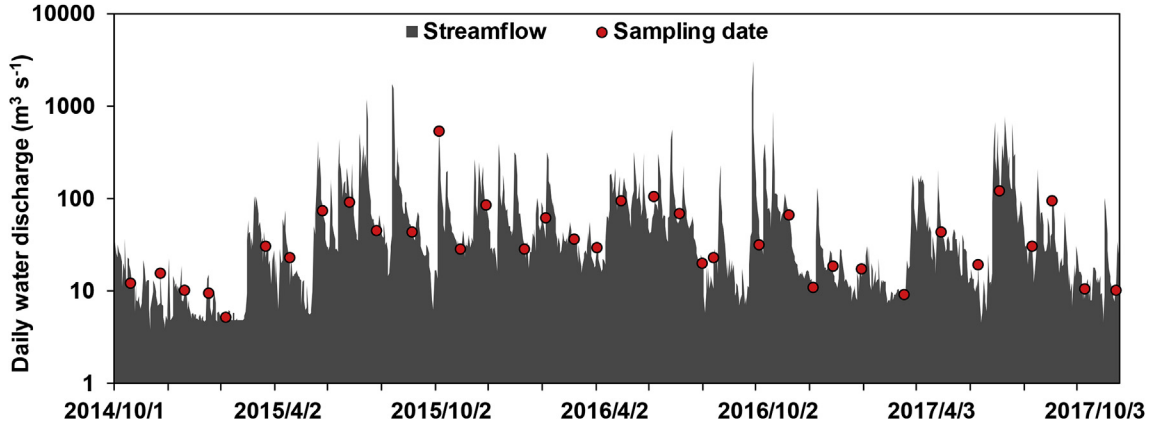

Fig. 2. Daily discharge and sampling dates in the Yongan watershed in 2014–2017.

2.3. Water quality and stable isotope analysis

Rainfall, groundwater and river water were analyzed for temperature (°C), pH, dissolved oxygen (DO), dissolved organic carbon (DOC), dissolved N_2O, total nitrogen (TN), total dissolved nitrogen, nitrate (NO_3^-) and ammonium (NH_4^+). Temperature, pH and DO were measured in the field using YSI electrodes (Xylem, New York, USA). All water samples were analyzed within 24 h; additional details on analytical methods are provided in Section 2 of SI.

Rainfall, groundwater and river water samples at the watershed outlet site were collected between October 2014 and October 2016 for isotopic analysis of $\delta^{18}O$-H_2O and $\delta^{2}H$-H_2O. Water isotopes (i.e., $\delta^{18}O$-H_2O and $\delta^{2}H$-H_2O) were determined using an isotope-ratio mass spectrometer (Delta V Advantage, Thermo Scientific). Two internal standards calibrated against VSMOW (Biscayne Aquifer Drinking Water (USGS45) and Lake Louise Drinking Water (USGS47)) were used to calibrate raw data and ensure long-term stability of analyses. The analytical precision was ±0.2‰ for $\delta^{18}O$-H_2O and ±1‰ for $\delta^{2}H$-H_2O.

Rainfall, groundwater and river water samples for $\delta^{15}N$-NO_3^- and $\delta^{18}O$-NO_3^- stable isotope analysis were collected from all catchments. Samples were frozen at −20 °C, and subsequently transported to the Environmental Stable Isotope Lab (Institute of Soil Science, Chinese Academy of Sciences, Nanjing, China) for analysis. Water samples were pre-processed by the chemical method of McIlvin and Altabet (2005) (See Section 2 of SI) to convert NO_3^- to gaseous N_2O for detection using a continuous-flow isotope ratio mass spectrometer (IRAM, Isoprime100). Isotope ratio values are reported in parts per thousand (‰) relative to atmospheric N_2 and Vienna Standard Mean Ocean water (VSMOW) for $\delta^{15}N$-NO_3^- and $\delta^{18}O$-NO_3^-, respectively (Kendall et al., 2007). Sample analysis had an average precision of 0.31‰ for $\delta^{15}N$-NO_3^- and 0.55‰ for $\delta^{18}O$-NO_3^-. The load-weighted mean (M_L) values for $\delta^{15}N$-NO_3^- and $\delta^{18}O$-NO_3^- were used to remove the NO_3^- load variability and emphasize biogeochemical influences (Voss et al., 2006). Although no groundwater sample was collected in the residential tributary (T_{res}), $\delta^{15}N$-NO_3^- and $\delta^{18}O$-NO_3^- values were estimated based on observed significant relationships between stable isotope values and area percentages of agricultural and residential land use across the three groundwater sampling wells (for ^{15}N-NO_3^-, $R^2 = 0.998$, $p < 0.05$; for ^{18}O-NO_3^-, $R^2 = 0.997$, $p < 0.05$, See Section 2 of SI). A similar approach was adopted in previous studies (Voss et al., 2006; Xue et al., 2009).

The combined isotopic signals of $\delta^{15}N$-NO_3^- and $\delta^{18}O$-NO_3^- were used to assess nitrification and denitrification processes. For denitrification, microbes utilize NO_3^- with lighter isotopes leading to enrichment of $\delta^{18}O$-NO_3^- and $\delta^{15}N$-NO_3^- at a ratio between 0.43 and 1.0 (Kendall et al., 2007; Xue et al., 2009; Ji et al., 2017). For nitrification, 2/3 of the O in the NO_3^- product is derived from ambient soil water and 1/3 from atmospheric O_2 (Kendall, 1998). As a result, the $\delta^{18}O$ values of NO_3^- derived from nitrification should range between −1.92‰ and 7.44‰, based on a $\delta^{18}O$ value of +23.5‰ for atmospheric O_2 and $\delta^{18}O$ values of −14.63‰ to −0.59‰ for precipitation (Yang et al., 2013).

2.4. River water source identification based on stable isotopes of water

Stable isotopes of water (^{2}H-H_2O and ^{18}O-H_2O) were examined to identify river water sources and better understand hydrological processes. Physically based stable isotopes serve as effective tracers with isotope fractionation producing a natural labeling effect that provides information on hydro-climate processes (McGuire and McDonnell, 2006). The sine wave regression method was conducted to estimate the young water fractions (F_{yw}). F_{yw} is defined as the proportion of the transit-time distribution younger than a threshold age (~0.2 year) (Kirchner, 2016). We calculated F_{yw} using sine wave regressions on the $\delta^{18}O$ (‰) time series (McGuire and

McDonnell, 2006) to determine the cosine and sine coefficients for precipitation and streamflow (See Section 3 of SI).

2.5. Riverine nitrogen source identification with stable isotope analysis in R (SIAR)

The Bayesian model (SIAR) was applied to estimate contributions of multiple NO_3^- sources in individual water samples (Parnell et al., 2010). Nitrogen pollution in rivers is mainly derived from point source (e.g., domestic, industry, and animal wastewaters) and non-point source (NPS) pollution pathways (Ongley et al., 2010). Driven by watershed hydrological processes, NPS pollution derived from various sources (e.g., chemical fertilizer, manure/sewage, and atmospheric deposition) will be transported to rivers through soil and groundwater (Griffiths et al., 2016). Due to hydrological and biogeochemical N legacy effects, it may take years to decades for some N sources to be transported to rivers through soil and groundwater in watersheds (Meals et al., 2010; Hamilton, 2012). Some long-term field experiments and watershed modeling results indicated that a very limited proportion (<2%) of annual N inputs was delivered to groundwater and surface water in the current year (Chen et al., 2018). Therefore, this study apportioned riverine N to groundwater, soil and wastewater to evaluate the efficacy of previous modeling results. Riverine N source apportionment analysis was conducted by SIAR at the outlet of Yongan watershed, agricultural tributary (T_{agr1}), forest tributary (T_{for}) and residential tributary (T_{res}). Groundwater and river water N isotope values were directly measured, while isotopic values for soil and wastewater N were obtained from published values for a nearby watershed (Ji et al., 2017). (See SIAR details in Section 3 of SI).

2.6. Statistical analysis

All correlation, regression and nonparametric analyses were performed using SPSS (version 17.0, SPSS, Chicago, IL, USA). One-way ANOVA with a LSD multiple comparisons test was used to examine differences in stable isotope values (δ^{15}N-NO_3^- and δ^{18}O-NO_3^-) among sites. Nonparametric tests were conducted to compare N concentrations among sites, since these values did not follow a normal distribution according to the Kolmogorov–Smirnov test.

3. Results and discussion

3.1. Spatial and temporal patterns in N dynamics

Across mainstem ($n = 143$) and tributary ($n = 164$) river waters, NO_3^- (Mean ± SD: 67 ± 18%) was the major component of TN and was significantly higher than NH_4^+ (15 ± 12%) and organic N (18 ± 15%). This pattern indicates the widespread role of NPS N pollution and highlights the importance of NO_3^- source identification (Ongley et al., 2010). Longitudinally, NO_3^- ($p < 0.001$) and NH_4^+ ($p < 0.001$) concentrations increased from upstream to downstream along the mainstem, with NO_3^- increasing by 60% and NH_4^+ by 300% (Fig. 3a), due to increasing N loads discharged from tributaries. Observed TN concentrations in tributaries dominated by residential and agricultural land use were significantly ($p < 0.01$) higher than those in the mainstem (Table 3), potentially caused by dilution effects. With respect to land-use, NO_3^- and NH_4^+ concentrations were significantly ($p < 0.001$) higher in tributaries dominated by residential and agricultural land use than those dominated by forests (Fig. 3c), which is consistent with previous studies in eastern and northern China (Sun et al., 2013; Yi et al., 2017).

There were no significant differences ($p > 0.05$) in NO_3^- concentrations among seasons in the mainstem; however, NH_4^+ concentrations were lower ($p < 0.05$) in summer (Fig. 3b). Similar seasonal patterns were observed in tributaries and groundwater (Fig. 3d and f). These results may be due to higher biological uptake and N transformation rates during the summer growing season (Sudduth et al., 2013; Griffiths et al., 2016). There was a significant positive relationship ($r = 0.25$, $p = 0.004$, $n = 131$) between water discharge and NO_3^- concentration in the mainstem, which became stronger ($r = 0.37$, $p < 0.001$, $n = 128$) when the three highest water discharge points (at least 2 times higher than other records) were removed (Fig. 4a). The trend of increasing NO_3^- concentration with increasing discharge further indicates the widespread role of NPS pollution (Lai et al., 2011). There was no significant relationship observed between water discharge and NO_3^- concentration in agricultural tributaries ($p = 0.296$, $n = 92$), which may suggest offsetting inputs of NPS N pollution load and dilution effects with increasing runoff/discharge (Fig. 4c). A significant negative relationship was found between water discharge and NO_3^- concentration in residential ($r = 0.25$, $p = 0.004$, $n = 131$) and forest ($r = 0.54$, $p = 0.01$, $n = 22$) tributaries (Fig. 4c), which may indicate a prominent dilution effect and less NPS pollution from residential and forest catchments (Kaushal et al., 2011). There were no significant differences in NH_4^+ concentrations between the low flow regime (30% lower bound of flow regime) and high flow regime (30% upper bound of flow regime) in mainstem ($p = 0.264$) or tributary ($p = 0.198$) sites (Fig. 4b and d, Table 3). This may be explained by enhanced biogeochemical processes during the low flow regime (Chen et al., 2013), which will lead to similarly low NH_4^+ concentrations to that in the high flow regime caused by dilution effects.

Observed N concentrations in groundwater samples were similar to those in river water (Fig. 3), suggesting the potential for relatively high groundwater contributions to rivers (Griffiths et al., 2016). As expected, NO_3^- concentrations in groundwater were significantly ($p < 0.001$) higher in catchments dominated by agriculture than at the watershed outlet and forest-dominated catchments. In contrast, NH_4^+ concentrations in groundwater were ~8–20 times lower than NO_3^- (Table 3). This is mainly due to cation exchange reactions in the soil, which limit NH_4^+ leaching mobility to groundwater as compared to NO_3^- (Swaney et al., 2012). Higher NH_4^+ concentrations in groundwater ($p < 0.05$) were observed at the outlet site and lower concentrations observed in catchments dominated by agriculture and forests (Fig. 3e). Comparing N concentrations between precipitation and river water (Fig. 3a and c), precipitation produced a dilution effect for NO_3^- while contributing an NH_4^+ source to rivers. Although no detailed spatial data were available in this study, high NH_4^+ concentrations in precipitation are generally derived from local fertilizer and manure volatilization (Kang et al., 2016) associated with excessive anthropogenic N inputs to lands in the Yongan watershed (Chen et al., 2016).

3.2. Investigating water and N cycling processes with stable isotopes

3.2.1. Water cycling characteristics and water source identification

Slopes of δ^2H-H_2O versus δ^{18}O-H_2O for river water (5.98) and groundwater (4.71) were lower than the local meteoric water line (8.23; Fig. 5). This result is associated with evapotranspiration, since ^{18}O will be more enriched than deuterium during evaporation (Gonfiantini, 1986), thereby increasing oxygen and hydrogen isotopic values generating a systematic deviation from LMWL (Sánchez-Murillo et al., 2015). The isotopic composition of river water (CV: 10.5–13.7% for δ^2H-H_2O; 8.9–11.8% for δ^{18}O-H_2O) was less variable than that of precipitation (CV: 91.4% for δ^2H-H_2O; 53.4% for δ^{18}O-H_2O), suggesting a substantial portion of river water may originate from groundwater and subsurface water sources. River water is a mixture of surface runoff, subsurface water and

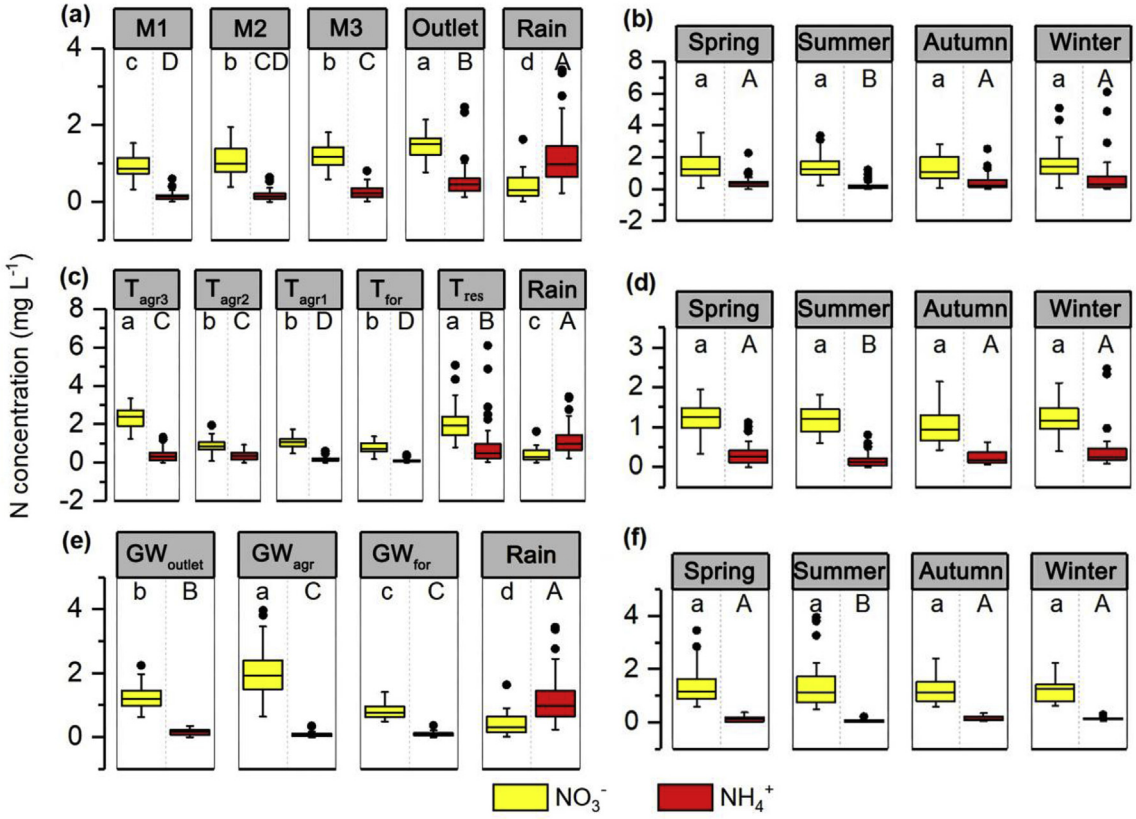

Fig. 3. Box plots for NO_3^- and NH_4^+ in (a) different mainstem sites and (b) in different seasons, (c) in different tributaries sites and (d) in different seasons, (e) in different groundwater sites, and (f) in different seasons. "M" represents the mainstem, "T" represents the tributary and "GW" represents groundwater. Subscript "agr" represents agricultural tributary, "for" represents forest tributary and "res" represents residential tributary. Box plots illustrate the 25th, 50th and 75th percentile; the whiskers indicate the 2.5th and 97.5th percentiles; and the points represent data outliers.

Table 3
Nitrogen concentrations and NO_3^- isotopic composition in the Yongan watershed during different flow regimes.

	TN (mg N L^{-1})	NO_3^- (mg N L^{-1})	NH_4^+ (mg N L^{-1})	δ^{15}N-NO_3^- (‰)	δ^{18}O-NO_3^- (‰)
Low flow regime					
Mainstem	1.75 ± 0.80	1.07 ± 0.38	0.35 ± 0.48	7.35 [a]	0.85 [a]
$Tributary_{agr}$	1.98 ± 1.39	1.20 ± 0.67	0.36 ± 0.35	8.27 [a]	2.76 [a]
$Tributary_{res}$	4.94 ± 3.09	2.78 ± 1.25	1.29 ± 1.33	9.03 [a]	0.48 [a]
$Tributary_{for}$	1.29 ± 0.35	0.99 ± 0.37	0.16 ± 0.14	2.25 [a]	−1.32 [a]
Medium flow regime					
Mainstem	1.67 ± 0.55	1.23 ± 0.42	0.24 ± 0.26	9.29 [a]	1.17 [a]
$Tributary_{agr}$	1.92 ± 0.81	1.47 ± 0.85	0.27 ± 0.24	9.05 [a]	2.22 [a]
$Tributary_{res}$	3.62 ± 2.00	2.15 ± 0.71	1.08 ± 1.70	12.66 [a]	1.03 [a]
$Tributary_{for}$	1.00 ± 0.22	0.68 ± 0.28	0.07 ± 0.05	4.54 [a]	1.49 [a]
High flow regime					
Mainstem	1.93 ± 1.58	1.18 ± 0.33	0.27 ± 0.19	6.00 [a]	0.81 [a]
$Tributary_{agr}$	2.38 ± 1.03	1.43 ± 0.71	0.33 ± 0.25	6.00 [a]	1.15 [a]
$Tributary_{res}$	2.69 ± 1.21	1.51 ± 0.32	0.56 ± 0.69	7.94 [a]	0.28 [a]
$Tributary_{for}$	1.20 ± 0.37	0.70 ± 0.27	0.11 ± 0.09	4.88 [a]	−0.76 [a]
Whole period					
Mainstem	1.78 ± 0.65	1.33 ± 0.70	0.30 ± 0.53	6.91 [a]	0.90 [a]
$Tributary_{agr}$	2.09 ± 1.07	1.39 ± 0.77	0.31 ± 0.27	6.87 [a]	1.49 [a]
$Tributary_{res}$	3.74 ± 2.74	2.11 ± 0.94	0.44 ± 0.75	9.36 [a]	0.51 [a]
$Tributary_{for}$	1.34 ± 0.32	0.77 ± 0.32	0.12 ± 0.10	4.64 [a]	−0.25 [a]
GW_{outlet}	1.69 ± 0.48	1.26 ± 0.41	0.15 ± 0.10	9.89 ± 5.57	2.45 ± 2.92
GW_{agr}	2.37 ± 0.89	2.01 ± 0.81	0.09 ± 0.08	8.16 ± 3.64	1.38 ± 2.73
GW_{for}	1.19 ± 0.30	0.80 ± 0.22	0.09 ± 0.08	5.97 ± 3.75	0.85 ± 3.68

Superscript "a" donates the load-weighted mean (M_L) values for δ^{15}N-NO_3^- and δ^{18}O-NO_3^-.

groundwater inputs having different ages (Howden et al., 2011). The overlapping water isotopic compositions between river water and groundwater (Fig. 5) indicate that groundwater (having a relatively older age) is an appreciable source of river water (Ji et al., 2017). Estimated baseflow (i.e., groundwater and slow subsurface flow) contributions based on the young water fractions (F_{yw}) for the

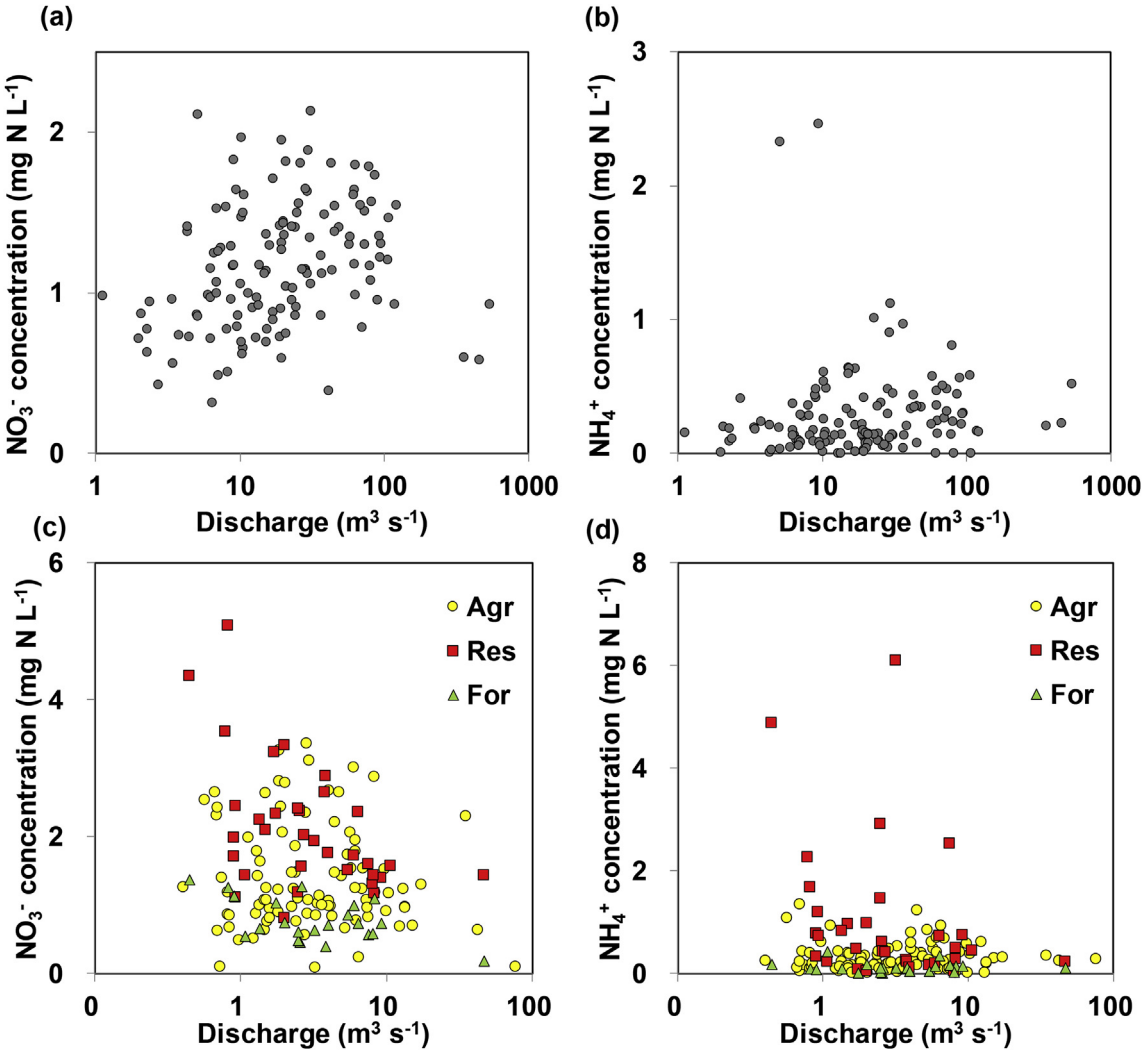

Fig. 4. Scatter plots for (a) NO_3^- and (b) NH_4^+ in mainstem, (c) NO_3^- and (d) NH_4^+ in agricultural (agr), residential (res) and forest (for) tributaries.

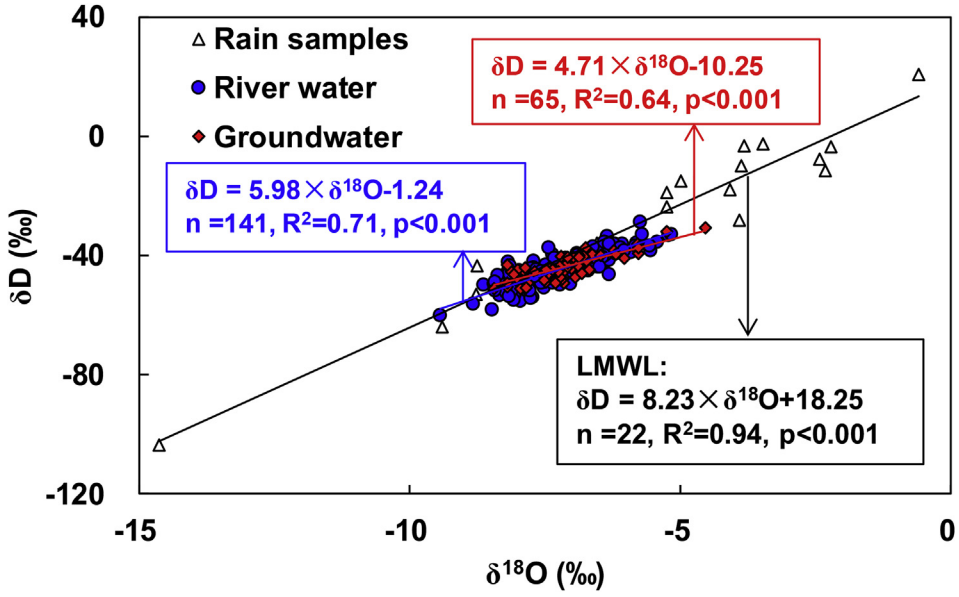

Fig. 5. Scatter plots for ^2H-H_2O and ^{18}O-H_2O in river water, groundwater and rainfall samples. Local meteoric water line (LMWL) is a regression line of measured stable isotopic composition from local rainfall samples.

sub-catchments and the entire Yongan watershed ranged from 79 to 85% of total streamflow (Fig. 8d). Such a high water contribution from baseflow to streamflow is consistent with ReNuMa model results for the Yongan watershed and has been commonly observed in many watersheds worldwide (Table 1). However, the use of watershed hydrological models in previous studies to quantify the fraction of different streamflow components has many challenges resulting from the high level of uncertainty associated with inherent limitations and assumptions of these methods (He and Lu, 2016). Instead, the F_{yw} method can accurately estimate streamflow components from the amplitude ratio of tracer cycles in precipitation and streamflow with a reported precision of a few percent (McGuire and McDonnell, 2006; Kirchner, 2016). Subsurface hydrological processes, with a particular focus on groundwater, could lead to a considerable lag effect in delivery of watershed nutrients to rivers (Meals et al., 2010). The lag effect from groundwater transport of NO_3^- derived years or decades ago could lead to an appreciable delay in the response of watershed N management activities (Chen et al., 2018; Van Meter et al., 2018).

3.2.2. N cycling process identification using NO_3^- stable isotopes

The ranges of $\delta^{18}O\text{-}NO_3^-$ and $\delta^{15}N\text{-}NO_3^-$ signatures between groundwater and river water were overlapping (Fig. 6), suggesting that groundwater may be a source of surface water NO_3^- (Griffiths et al., 2016). The $\delta^{18}O\text{-}NO_3^-$ and $\delta^{15}N\text{-}NO_3^-$ source signatures indicated (Fig. 6d) that direct N inputs from soil and chemical fertilizer were potentially limited in agricultural tributaries, but soil N was a potentially major N source in the forest tributary. In contrast, wastewater was the potentially dominant N contributor in the residential tributary (Fig. 6d). These results are similar to previous studies and emphasize human impacts on N dynamics (Xia et al., 2017; Yi et al., 2017). Greater than 80% of river water (including mainstem and tributaries) $\delta^{18}O$ values for NO_3^- (Fig. 6b and d) fall within the range expected for NO_3^- formed as a product of nitrification (Yang et al., 2013). Among different tributaries, $\delta^{15}N\text{-}NO_3^-$ values for residential land were significantly higher than those for agricultural ($p < 0.001$) and forested tributaries ($p = 0.002$) (Table 3). Estimated slopes between $\delta^{15}N\text{-}NO_3^-$ and $\delta^{18}O$ in the mainstem (slope = 0.23; $R^2 = 0.09$, $p = 0.001$, $n = 131$) and tributaries (slope = 0.24; $R^2 = 0.12$, $p < 0.001$, $n = 147$) were considerably lower than slopes expected for waters experiencing considerable denitrification (slopes between 0.43 and 1.0) (Xue et al., 2009; Ji et al., 2017; Xia et al., 2017). Although there was no significant decrease in N concentrations during spring and winter compared to other seasons (Fig. 3b), a positive relationship ($R^2 = 0.39$, $p = 0.003$, $n = 20$) with a slope of 0.85 was found during the low flow regime in spring and winter (Fig. 6a). This isotopic relationship may suggest the potential for denitrification (Kendall et al., 2007). However, no significant relationship ($p = 0.814$, $n = 22$) was observed between $\delta^{15}N\text{-}NO_3^-$ and $\delta^{18}O\text{-}NO_3^-$ in the forest tributary (Fig. 6b). Although a positive relationship between $\delta^{15}N\text{-}NO_3^-$ and $\delta^{18}O\text{-}NO_3^-$ in agricultural ($R^2 = 0.15$, $p < 0.001$, slope = 0.28, $n = 92$) and residential ($R^2 = 0.16$, $p = 0.020$, slope = 0.29, $n = 33$) tributaries was observed (Fig. 6b), the slopes were too low to provide strong evidence for denitrification. The weak denitrification signatures may result from high DO concentrations (6.76 ± 1.70 mg L^{-1}) in river waters, which were much higher than expected to support denitrification (<2 mg L^{-1}, Rivett et al., 2008). Overall, these results suggest that nitrification rather than denitrification is the likely dominant N transformation process in Yongan watershed (Yang et al., 2013; Ji et al., 2017).

For groundwater samples, the slope (0.14) for the $\delta^{15}N\text{-}NO_3^-$ versus $\delta^{18}O\text{-}NO_3^-$ relationship was lower than the expected denitrification slopes (Fig. 6f). NO_3^- produced through nitrification combines with relatively low $\delta^{18}O$ from water that could conceal the effects of denitrification on the $\delta^{15}N\text{-}NO_3^-$ versus $\delta^{18}O\text{-}NO_3^-$ relationship (Osaka et al., 2010). There was also no significant negative relationship between $\ln[NO_3^-]$ and $\delta^{15}N\text{-}NO_3^-$, which would be expected due to the NO_3^- loss that accompanies the increase of $\delta^{15}N\text{-}NO_3^-$ during denitrification (Kendall et al., 2007). Notably, mixed N sources might obscure the groundwater nitrate concentration vs $\delta^{15}N\text{-}NO_3^-$ and $\delta^{15}N\text{-}NO_3^-$ vs $\delta^{18}O\text{-}NO_3^-$ relationships. In China, N leaching from land-applied fertilizer and manure (e.g., domestic and animal wastes) and the prevalence of leaky septic systems are considered major sources of groundwater NO_3^- in agricultural and residential areas (Lu et al., 2008). In addition, the legacy effect may also have a considerable influence on isotopic signals, as well as the groundwater nitrate concentration vs $\delta^{15}N\text{-}NO_3^-$ relationship and $\delta^{15}N\text{-}NO_3^-$ vs $\delta^{18}O\text{-}NO_3^-$ relationship, since N in water samples is a mixture from different sources and times (Howden et al., 2011).

Measured dissolved N_2O concentrations in groundwater (3.51 ± 3.17 μg L^{-1}) were much higher ($p < 0.001$) than surface waters (0.58 ± 0.35 μg L^{-1}) (Fig. 7). Higher dissolved N_2O concentrations in the groundwater of outlet and T_{agr1} sites than for T_{for} ($p < 0.001$, Fig. 7) suggest that N_2O production (and thereby nitrification and denitrification) is more prevalent in agricultural lands and near the outlet site than for forested sites. Comparatively lower DO concentrations (3.71 ± 1.46 mg L^{-1}) measured in $Outlet_{gw}$ and GW_{agr} were more favorable for denitrification than those measured in surface waters (Rivett et al., 2008). Two observations during the low flow regime (January in 2015 and 2016) had very high $\delta^{15}N\text{-}NO_3^-$ values [>20‰, exceeded the maximum groundwater $\delta^{15}N\text{-}NO_3^-$ observed in nearby regions by Xue et al. (2009), Fig. 6e], which may be influenced by random human activities or analytical errors. When these two high $\delta^{15}N\text{-}NO_3^-$ values were removed, a significant relationship ($R^2 = 0.33$, $p = 0.001$, slope = 0.48, $n = 31$) between $\delta^{15}N\text{-}NO_3^-$ and $\delta^{18}O\text{-}NO_3^-$ was observed for $Outlet_{gw}$ (Fig. 6e), implying a potential for denitrification. Since denitrification is strongly influenced by DOC availability (Ben Maamar et al., 2015; Pinay et al., 2015), $\delta^{15}N\text{-}NO_3^-$ and $\delta^{18}O\text{-}NO_3^-$ data for GW_{outlet} and GW_{agr} were separated by DOC concentrations for further analysis. The upper 50% DOC concentration group showed a significant relationship between $\delta^{15}N\text{-}NO_3^-$ and $\delta^{18}O\text{-}NO_3^-$ ($R^2 = 0.71$, $p = 0.001$, slope = 0.62, $n = 12$). These results suggest that denitrification is likely occurring along the groundwater flowpath. Additional studies are warranted to assess the importance of denitrification in groundwater across various land uses at the watershed scale.

3.3. N source identification in river water

For the entire Yongan watershed, SIAR estimates indicated that groundwater contributed $43 \pm 17\%$ of the river NO_3^- load, followed by soil N ($33 \pm 8\%$) and wastewater N ($25 \pm 15\%$) (Fig. 8a). The high contributions from soil and groundwater confirm that NPS pollution was the dominant contributor to riverine N load. The sum of estimated N contributions from groundwater ($43 \pm 17\%$) and soil ($33 \pm 8\%$) was virtually identical to the 79% baseflow contribution for the entire watershed (Fig. 8d). Corresponding to estimated baseflow contributions across the three sub-catchments (i.e., 85%, 84%, and 81%, Fig. 8d), groundwater N contributed to $52 \pm 17\%$, $41 \pm 18\%$ and $37 \pm 16\%$ of riverine NO_3^- loads in agricultural residential and forest tributaries, respectively (Fig. 8a). These results imply that slow flow through the soil zone and groundwater system is an important source of both riverine NO_3^- and water. These estimates are consistent with a previous modeling study that predicted NPS and point sources contributed ~72% and ~18% of riverine N load during the 2000s in the Yongan watershed, respectively (Hu et al., 2018). Additional modeling results from the Yongan watershed estimated that >70% of the N exported by rivers was derived

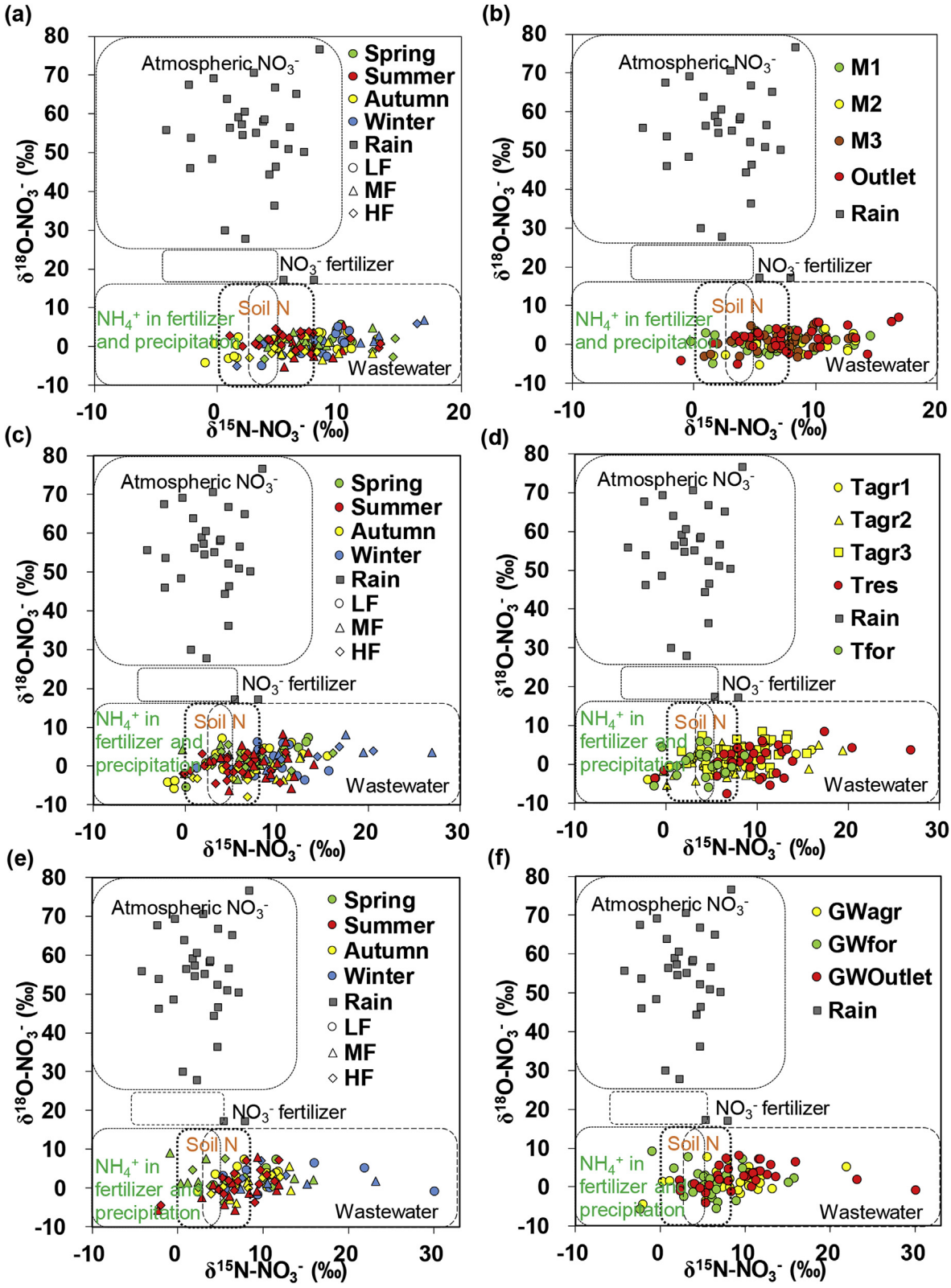

Fig. 6. Dual $\delta^{15}N\text{-}NO_3^-$ and $\delta^{18}O\text{-}NO_3^-$ in rainfall and (a) mainstem water samples in different seasons and flow regimes, (b) mainstem water samples at different sampling sites, (c) tributaries water samples in different seasons and flow regimes, (d) tributaries water samples at different sampling sites, (e) groundwater in different seasons and flow regimes and (f) groundwater at different sampling sites. Area shows the range of the $\delta^{15}N\text{-}NO_3^-$ and $\delta^{18}O\text{-}NO_3^-$ values from Xue et al. (2009), Kaushal et al. (2011) and Yi et al. (2017). Circle in (a), (c) and (e) represents low flow regime (LF = lowest 30% of flows), triangle represents medium flow regime (MF) and rhombus represents high flow regime (HF = upper 30% of flows). T_{agr} is agricultural tributary, T_{res} is residential tributary, T_{for} is forest tributary and GW is groundwater.

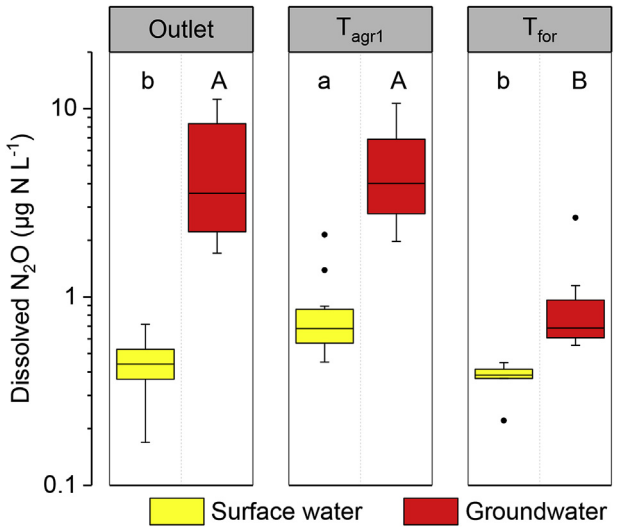

Fig. 7. Box plots for dissolved N_2O-N concentrations in surface water and groundwater at outlet site of Yongan watershed, agricultural tributary (T_{agr1}) and forest tributary (T_{for}).

from soil and groundwater N pools (Chen et al., 2014a, 2016, 2014b). High soil and groundwater N contributions to riverine NO_3^- loads are widely reported in watersheds worldwide from models and water quality monitoring (Table 1). This study integrated information from multiple isotope tracers, providing independent methods for verifying and understanding N transformation and transport pathways. Future measurements of ^3H, CFCs, and sulfur hexafluoride (SF_6) (Sanford and Pope, 2013; Tesoriero et al., 2013) may further refine estimates for the ages of groundwater and surface water providing additional verification.

The dominant contributions of soil and groundwater N to riverine N implies the potential for a considerable N leaching lag effect at the watershed scale (Meals et al., 2010; Sanford and Pope, 2013; Hamilton, 2012; Van Meter et al., 2017, 2018). In terms of previous modeling studies, there was ~10 years of lag time between N inputs from various NPS inputs (e.g., fertilizer, biological fixation, atmospheric deposition) and riverine N export in Yongan watershed due to long residence times for hydrologic flowpaths and biogeochemical transformations (Chen et al., 2014b, 2016, 2014a). Previous studies reported relatively long lag times for nitrate transport due to hydrological (~1 to >50 years) and biogeochemical processes (<10—~100 years) in watersheds worldwide (Meals et al., 2010; Hamilton, 2012; Chen et al., 2018; Dupas et al., 2018). These N-leaching lag effects introduce considerable uncertainty in apportioning riverine nitrate to conventional sources (e.g., atmospheric deposition, chemical fertilizer, soil N, manure/sewage).

As expected, there were considerable differences in N source components across different catchments (Fig. 8). For the residential tributary, wastewater N was estimated to contribute the highest riverine NO_3^- proportion (~35%), which is consistent with the higher population density (828 capita km^{-2}) and domestic animal numbers (136 capita km^{-2}) observed in the residential tributary catchment compared to the other catchments (<300 capita km^{-2} and <120 capita km^{-2}) (Table 2). For the agricultural tributary, groundwater N was estimated to contribute nearly 60% of the riverine NO_3^- load, with soil and wastewater contributing ~35% and ~5%, respectively. In contrast, N sources in the forest tributary were dominated by soil N (>50%) and groundwater (~40%). The lower groundwater N contribution in the forest catchment can be explained by significantly lower groundwater NO_3^- concentrations in forest-dominated catchments (0.80 ± 0.22 mg N L^{-1}) compared to agricultural catchments (2.01 ± 0.81 mg N L^{-1}) (Fig. 3e). The

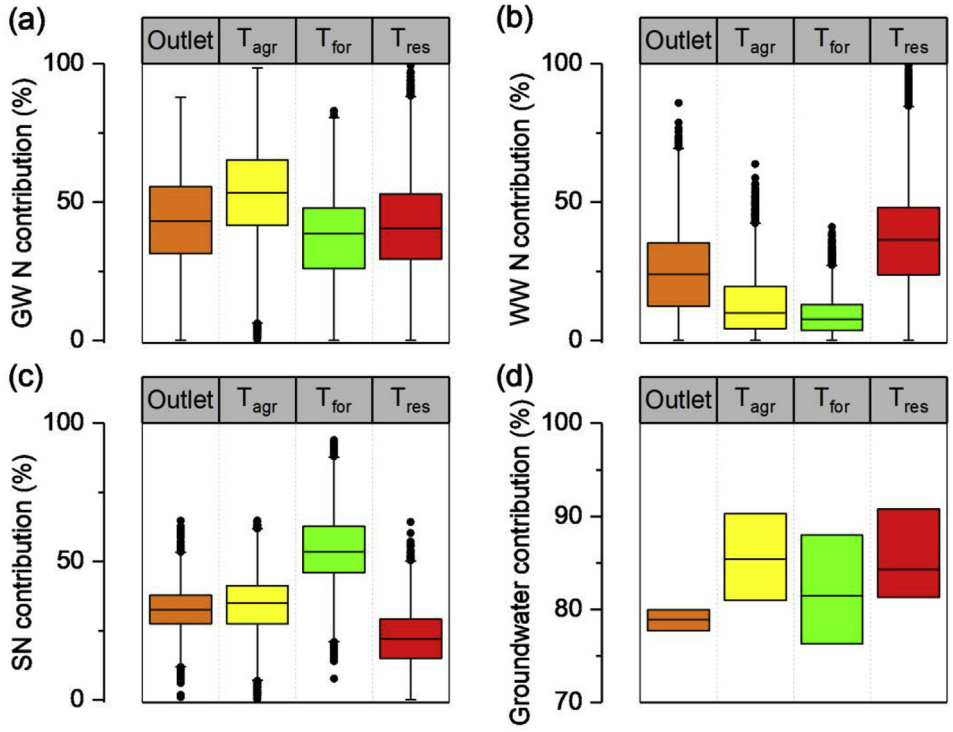

Fig. 8. Box plots for (a) the contribution of groundwater, (b) wastewater N and (c) soil N to riverine NO_3^- in at the Yongan watershed outlet (Outlet), agricultural tributary (T_{agr}) and forest tributary (T_{for}); (d) water contribution from groundwater in different catchments based on sine wave regressions. Box plots in (a), (b), (c) illustrate the 25th, 50th and 75th percentile; the whiskers indicate the 2.5th and 97.5th percentiles; and the points represent data outliers. Box plots in (d) illustrate the 2.5th, mean values and 97.5th percentiles.

paddy field proportion in T_{agr1} (5.6%) was much higher than that in T_{for} (1.5%), which lead to higher fertilizer application and higher water infiltration into subsurface flow and/or groundwater hydrologic pathways (Table 2). For example, ~380 mm yr^{-1} of water infiltration combined with high soil N levels contributed considerable NO_3^- leaching to groundwater in paddy fields of the nearby Taihu region (Xu et al., 2017). The different N source (e.g., soil, groundwater and wastewater) contributions among different subcatchments are consistent with results observed in nearby watersheds in eastern China (Xing and Liu, 2016; Xia et al., 2017). Overall, the differences distinguished for N contributions among tributaries are strongly related to the influence of land use on N fate and transport.

3.4. Implications for river N pollution control

Results of this study were mutually supported by hydrochemistry, multiple stable isotopes (^{15}N-NO_3^-/^{18}O-NO_3^- and ^2H-H_2O/^{18}O-H_2O), dissolved N_2O concentrations, and previous modeling results, thereby providing an integrated approach for exploring and quantifying watershed N transformation and transport pathways. This study provides watershed managers with important information for making science-based decisions on N pollution control strategies. Since NPS pollution dominated in Yongan watershed, management strategies for controlling riverine N pollution should be focused on reducing NPS pollution (Fig. 8a and c). NPS N pollution can be controlled by several management strategies, such as improved irrigation and nutrient management, reduced-tillage with enhanced crop residue cover, seasonal cover crops, and vegetative buffer zones between croplands and rivers (Ji et al., 2017). To address high wastewater N contributions in residential catchments, centralized collection of wastes from individual households, currently having marginal septic systems, is critical for reducing N pollution and several other human-health hazards. For example, efficient wastewater collection and centralized treatment systems and/or artificial wetlands should be implemented to efficiently reduce N pollution loads from domestic and animal wastes (Chen et al., 2013).

Results of this study combined with previous modeling studies (Chen et al., 2014a, 2014b; Hu et al., 2018) confirm the potential for high NO_3^- contributions from groundwater and soil N pools (Fig. 8), implying a N-leaching legacy effect in the Yongan watershed. Therefore, reduction of N inputs from various sources (e.g., atmospheric deposition, chemical fertilizer, biological fixation) may not be immediately recognized as decreased riverine N loads (Meals et al., 2010). Instead, measures aimed at reducing soil and groundwater N pools that contribute appreciable NO_3^- loads should be considered, in addition to measures to reduce anthropogenic input sources. Since riparian and hyporheic zones are recognized as hot spots for NO_3^- removal, restoration of stream and riparian zones is a compelling strategy for enhancing groundwater NO_3^- removal by denitrification (Boano et al., 2014). Possible strategies for enhancing in-stream denitrification include increasing river water residence times, restoring floodplains and increasing microbially available carbon (Hester and Gooseff, 2010). Permeable reactive barrier technology also provides a promising way for sustainable *in situ* groundwater restoration, which makes use of *in situ* groundwater flow to bring N pollutants in contact with reactive materials for NO_3^- removal by microbial denitrification (Liu et al., 2013; Obiri-Nyarko et al., 2014). To reduce the soil N pool contribution to legacy N in agricultural soils, sustainable nutrient management measures should be integrated to optimize uptake of legacy nutrients and reduce new fertilizer inputs (Chen et al., 2018) and incorporate perennial vegetation to more efficiently sequester nutrients while also providing a source of forage or biofuels (Van Meter et al., 2017; Thomas and Abbott, 2018).

4. Conclusion

This study combined 3-years of multiple stable isotopes, hydrologic, water chemistry and nitrous oxide measurements as well as N sources identified in previous modeling studies to assess N dynamics and riverine N sources in the Yongan Watershed. This investigation provides a reliable and integrated approach for verifying and understanding N pollution legacy effects observed in many watersheds worldwide. Information from $\delta^{15}N$-NO_3^- and $\delta^{18}O$-NO_3^- indicated that riverine N dynamics were regulated by contributing sources, nitrification and denitrification, as well as hydrological processes. Information from ^2H-H_2O and ^{18}O-H_2O indicated that slow subsurface and groundwater flows, accounting for >75% of river water discharge, were potentially major hydrologic pathways for N delivery to the river. Riverine NO_3^- source contributions varied with dominant land-use types, with the highest contributions from groundwater (60%), wastewater (35%), and soil (50%) occurring in agricultural, residential and forest catchments, respectively. High N contributions from groundwater and soil N pools imply considerable potential for nutrient leaching legacy effects. Results highlight that river N pollution control requires particular attention to groundwater restoration and soil N management in addition to N input control strategies. Several future research needs were identified to better understand the fate and transport of N through the soil and groundwater systems, as these are the dominant N pools regulating river N pollution.

Declaration of interests

The authors declare that they have no known competing financial interests or personal relationships that could have appeared to influence the work reported in this paper.

Acknowledgement

We thank local government departments for providing data critical for this investigation. This work was supported by the National Natural Science Foundation of China (41877465 and 51679210), Zhejiang Provincial Natural Science Foundation of China (LR19D010002), and National Key Research and Development Program of China (2017YFD0800101).

Appendix A. Supplementary data

Supplementary data to this article can be found online at https://doi.org/10.1016/j.watres.2018.11.082.

References

Abbott, B.W., Baranov, V., Mendoza-Lera, C., Nikolakopoulou, M., Harjung, A., Kolbe, T., Balasubramanian, M.N., Vaessen, T.N., Ciocca, F., Campeau, A., Wallin, M.B., Romeijn, P., Antonelli, M., Gonçalves, J., Datry, T., Laverman, A.M., de Dreuzy, J.R., Hannah, D.M., Krause, S., Oldham, C., Pinay, G., 2016. Using multi-tracer inference to move beyond single-catchment ecohydrology. Earth Sci. Rev. 160, 19–42.

Ben Maamar, S., Aquilina, L., Quaiser, A., Pauwels, H., Michon-Coudouel, S., Vergnaud-Ayraud, V., Labasque, T., Roques, C., Abbott, B.W., Dufresne, A., 2015. Groundwater isolation governs chemistry and microbial community structure along hydrologic flowpaths. Front. Microbiol. 6, 1457.

Boano, F., Harvey, J.W., Marion, A., Packman, A.I., Revelli, R., Ridolfi, L., Wörman, A., 2014. Hyporheic flow and transport processes: mechanisms, models, and biogeochemical implications. Rev. Geophys. 52 (4), 603–679.

Borah, D.K., Bera, M., 2004. Watershed-scale hydrologic and nonpoint-source pollution models: review of applications. Trans. ASAE (Am. Soc. Agric. Eng.) 47 (3), 789.

Bouraoui, F., Grizzetti, B., 2014. Modelling mitigation options to reduce diffuse nitrogen water pollution from agriculture. Sci. Total Environ. 468, 1267–1277.

Cherkauer, D.S., McKereghan, P.F., Schalch, L.H., 1992. Delivery of chloride and nitrate by ground water to the Great Lakes: case study for the Door Peninsula, Wisconsin. Ground Water 30 (6), 885–894.
Chen, D.J., Dahlgren, R.A., Lu, J., 2013. A modified load apportionment model for identifying point and diffuse source nutrient inputs to rivers from stream monitoring data. J. Hydrol. 501, 25–34.
Chen, D.J., Huang, H., Hu, M.P., Dahlgren, R.A., 2014a. Influence of lag effect, soil release, and climate change on watershed anthropogenic nitrogen inputs and riverine export dynamics. Environ. Sci. Technol. 48 (10), 5683–5690.
Chen, D.J., Hu, M.P., Dahlgren, R.A., 2014b. A dynamic watershed model for determining the effects of transient storage on nitrogen export to rivers. Water Resour. Res. 50 (10), 7714–7730.
Chen, D.J., Hu, M.P., Guo, Y., Dahlgren, R.A., 2016. Modeling forest/agricultural and residential nitrogen budgets and riverine export dynamics in catchments with contrasting anthropogenic impacts in eastern China between 1980–2010. Agric. Ecosyst. Environ. 221, 145–155.
Chen, D.J., Shen, H., Hu, M.P., Wang, J.H., Zhang, Y.F., Dahlgren, R.A., 2018. Legacy nutrient dynamics at the watershed scale: principles, modeling, and implications. Adv. Agron. 149, 237–313.
Chen, L., 2013. Modeling of the Water Flow and Nitrate Transport in the Shallow Aquifer of the Shaying River Basin and its Contribution to River Pollution. Doctoral Dissertation. NanJing University, NanJing.
Covino, T., 2017. Hydrologic connectivity as a framework for understanding biogeochemical flux through watersheds and along fluvial networks. Geomorphology 277, 133–144.
Dupas, R., Minaudo, C., Gruau, G., Ruiz, L., Gascuel-Odoux, C., 2018. Multidecadal trajectory of riverine nitrogen and phosphorus dynamics in rural catchments. Water Resour. Res. 54 (8), 5327–5340.
Galloway, J.N., Dentener, F.J., Capone, D.G., Boyer, E.W., Howarth, R.W., Seitzinger, S.P., Asner, G.P., Cleveland, C.C., Green, P.A., Holland, E.A., Karl, D.M., Michaels, A.F., Porter, J.H., Townsend, A.R., Vöosmarty, C.J., 2004. Nitrogen cycles: past, present, and future. Biogeochemistry 70 (2), 153–226.
Gonfiantini, R., 1986. Environmental Isotopes in Lake Studies. Handbook of Environmental Isotope Geochemistry; the Terrestrial Environment. Elsevier B.V., pp. 113–168
Griffiths, N.A., Jackson, C.R., McDonnell, J.J., Klaus, J., Du, E., Bitew, M.M., 2016. Dual nitrate isotopes clarify the role of biological processing and hydrologic flow paths on nitrogen cycling in subtropical low-gradient watersheds. J. Geophys. Res. - Biogeo. 121 (2), 422–437.
Hamilton, S.K., 2012. Biogeochemical time lags may delay responses of streams to ecological restoration. Freshw. Biol. 57 (s1), 43–57.
He, S.J., Lu, J., 2016. Contribution of baseflow nitrate export to non-point source pollution. Sci. China Earth Sci. 59 (10), 1912–1929.
Hester, E.T., Gooseff, M.N., 2010. Moving beyond the banks: hyporheic restoration is fundamental to restoring ecological services and functions of streams. Environ. Sci. Technol. 44, 1521–1525.
Howden, N.J.K., Burt, T.P., Mathias, S.A., Worrall, F., Whelan, M.J., 2011. Modelling long-term diffuse nitrate pollution at the catchment-scale: data, parameter and epistemic uncertainty. J. Hydrol. 403 (3–4), 337–351.
Hu, M.P., Liu, Y.M., Wang, J.H., Dahlgren, R.A., Chen, D.J., 2018. A modification of the Regional Nutrient Management model (ReNuMa) to identify long-term changes in riverine nitrogen sources. J. Hydrol. 561, 31–42.
Janke, B.D., Finlay, J.C., Hobbie, S.E., Baker, L.A., Sterner, R.W., Nidzgorski, D., Wilson, B.N., 2014. Contrasting influences of stormflow and baseflow pathways on nitrogen and phosphorus export from an urban watershed. Biogeochemistry 121 (1), 209–228.
Ji, X.L., Xie, R.T., Hao, Y., Lu, J., 2017. Quantitative identification of nitrate pollution sources and uncertainty analysis based on dual isotope approach in an agricultural watershed. Environ. Pollut. 229, 586–594.
Kang, Y., Liu, M., Song, Y., Huang, X., Yao, H., Cai, X., Zhang, H., Kang, L., Liu, X., Yan, X., He, H., Shao, M., Zhu, T., 2016. High-resolution ammonia emissions inventories in China from 1980-2012. Atmos. Chem. Phys. 16 (4), 2043–2058.
Kaushal, S.S., Groffman, P.M., Band, L.E., Elliott, E.M., Shields, C.A., Kendall, C., 2011. Tracking nonpoint source nitrogen pollution in human-impacted watersheds. Environ. Sci. Technol. 45 (19), 8225–8232.
Kendall, C., 1998. Tracing nitrogen sources and cycling in catchments. In: Isotope Tracers in Catchment Hydrology. Elsevier B.V., pp. 519–576
Kendall, C., Elliott, E.M., Wankel, S.D., 2007. Tracing Anthropogenic Inputs of Nitrogen to Ecosystems. Stable Isotopes in Ecology and Environmental Science, second ed. Blackwell Publishing Ltd., pp. 375–449
Kim, G., Lee, H., Lim, Y., Jung, M., Kong, D., 2010. Baseflow contribution to nitrates in an urban stream in Daejeon, Korea. Water Sci. Technol. 61 (12), 3216–3220.
Kirchner, J.W., 2016. Aggregation in environmental systems–Part 1: seasonal tracer cycles quantify young water fractions, but not mean transit times, in spatially heterogeneous catchments. Hydrol. Earth Syst. Sci. 20 (1), 279.
Lai, Y.C., Yang, C.P., Hsieh, C.Y., Wu, C.Y., Kao, C.M., 2011. Evaluation of non-point source pollution and river water quality using a multimedia two-model system. J. Hydrol. 409 (3–4), 583–595.
Liu, S.J., Zhao, Z.Y., Li, J., Wang, J., Qi, Y., 2013. An anaerobic two-layer permeable reactive biobarrier for the remediation of nitrate-contaminated groundwater. Water Res. 47 (16), 5977–5985.
Lu, Y., Tang, C., Chen, J., Sakura, Y., 2008. Impact of septic tank systems on local groundwater quality and water supply in the Pearl River Delta, China: case study. Hydrol. Process. 22 (3), 443–450.
McGuire, K.J., McDonnell, J.J., 2006. A review and evaluation of catchment transit time modeling. J. Hydrol. 330, 543–563.
McIlvin, M.R., Altabet, M.A., 2005. Chemical conversion of nitrate and nitrite to nitrous oxide for nitrogen and oxygen isotopic analysis in freshwater and seawater. Anal. Chem. 77 (17), 5589–5595.
Minet, E.P., Goodhue, R., Meier-Augenstein, W., Kalin, R.M., Fenton, O., Richards, K.G., Coxon, C.E., 2017. Combining stable isotopes with contamination indicators: a method for improved investigation of nitrate sources and dynamics in aquifers with mixed nitrogen inputs. Water Res. 124, 85–96.
Moatar, F., Abbott, B.W., Minaudo, C., Curie, F., Pinay, G., 2017. Elemental properties, hydrology, and biology interact to shape concentration-discharge curves for carbon, nutrients, sediment, and major ions. Water Resour. Res. 53, 1270–1287.
Meals, D.W., Dressing, S.A., Davenport, T.E., 2010. Lag time in water quality response to best management practices: a review. J. Environ. Qual. 39 (1), 85–96.
Obiri-Nyarko, F., Grajales-Mesa, S.J., Malina, G., 2014. An overview of permeable reactive barriers for in situ sustainable groundwater remediation. Chemosphere 111, 243–259.
Ohte, N., 2013. Tracing sources and pathways of dissolved nitrate in forest and river ecosystems using high-resolution isotopic techniques: a review. Ecol. Res. 28 (5), 749–757.
Ongley, E.D., Xiaolan, Z., Tao, Y., 2010. Current status of agricultural and rural non-point source pollution assessment in China. Environ. Pollut. 158 (5), 1159–1168.
Osaka, K., Ohte, N., Koba, K., Yoshimizu, C., Katsuyama, M., Tani, M., Tayasu, I., Nagata, T., 2010. Hydrological influences on spatiotemporal variations of $\delta^{15}N$ and $\delta^{18}O$ of nitrate in a forested headwater catchment in central Japan: denitrification plays a critical role in groundwater. J. Geophys. Res. - Biogeo. 115, G02021. https://doi.org/10.1029/2009JG000977.
Parnell, A.C., Inger, R., Bearhop, S., Jackson, A.L., 2010. Source partitioning using stable isotopes: coping with too much variation. PLoS One 5 (3) e9672.
Pionke, H., Gburek, W., Sharpley, A., Schnabel, R., 1996. Flow and nutrient export patterns for an agricultural hill-land watershed. Water Resour. Res. 32, 1795–1804.
Pinay, G., Peiffer, S., De Dreuzy, J.R., Krause, S., Hannah, D.M., Fleckenstein, J.H., Sebilo, M., Bishop, K., Hubert-Moy, L., 2015. Upscaling nitrogen removal capacity from local hotspots to low stream orders' drainage basins. Ecosystems 18 (6), 1101–1120.
Rivett, M.O., Buss, S.R., Morgan, P., Smith, J.W., Bemment, C.D., 2008. Nitrate attenuation in groundwater: a review of biogeochemical controlling processes. Water Res. 42 (16), 4215–4232.
Sanford, W.E., Pope, J.P., 2013. Quantifying groundwater's role in delaying improvements to Chesapeake Bay water quality. Environ. Sci. Technol. 47 (23), 13330–13338.
Sánchez-Murillo, R., Brooks, E.S., Elliot, W.J., Boll, J., 2015. Isotope hydrology and baseflow geochemistry in natural and human-altered watersheds in the Inland Pacific Northwest, USA. Isot. Environ. Health Stud. 51, 231–254.
Schilling, K., Zhang, Y.K., 2004. Baseflow contribution to nitrate-nitrogen export from a large, agricultural watershed, USA. J. Hydrol. 295, 305–316.
Sudduth, E.B., Perakis, S.S., Bernhardt, E.S., 2013. Nitrate in watersheds: straight from soils to streams? J. Geophys. Res. - Biogeo. 118 (1), 291–302.
Sun, R., Chen, L., Chen, W., Ji, Y., 2013. Effect of land-use patterns on total nitrogen concentration in the upstream regions of the Haihe River Basin, China. Environ. Manag. 51 (1), 45–58.
Swaney, D.P., Hong, B., Ti, C., Howarth, R.W., Humborg, C., 2012. Net anthropogenic nitrogen inputs to watersheds and riverine N export to coastal waters: a brief overview. Curr. Opin. Env. Sust. 4 (2), 203–211.
Tesoriero, A.J., Duff, J.H., Saad, D.A., Spahr, N.E., Wolock, D.M., 2013. Vulnerability of streams to legacy nitrate sources. Environ. Sci. Technol. 47 (8), 3623–3629.
Thomas, Z., Abbott, B.W., 2018. Hedgerows reduce nitrate flux at hillslope and catchment scales via root uptake and secondary effects. J. Contam. Hydrol. 215, 51–61.
Van Meter, K.J., Basu, N.B., Van Cappellen, P., 2017. Two centuries of nitrogen dynamics: legacy sources and sinks in the Mississippi and Susquehanna River Basins. Global Biogeochem. Cycles 31 (1), 2–23.
Van Meter, K.J., Van Cappellen, P., Basu, N.B., 2018. Legacy nitrogen may prevent achievement of water quality goals in the Gulf of Mexico. Science 360 (6387), 427–430.
Voss, M., Deutsch, B., Elmgren, R., Humborg, C., Kuuppo, P., Pastuszak, M., Rolff, C., Schulte, U., 2006. River biogeochemistry and source identification of nitrate by means of isotopic tracers in the Baltic Sea catchments. Biogeosci. Discuss. 3 (3), 475–511.
Wang, Y., Liu, X.L., Li, Y., Liu, F., Shen, J.L., Li, Y.Y., Ma, Q.M., Yin, J., Wu, J.S., 2015. Rice agriculture increases base flow contribution to catchment nitrate loading in subtropical central China. Agric. Ecosyst. Environ. 214, 86–95.
Wellen, C., Kamran-Disfani, A.R., Arhonditsis, G.B., 2015. Evaluation of the current state of distributed watershed nutrient water quality modeling. Environ. Sci. Technol. 49 (6), 3278–3290.
Xia, Y.Q., Li, Y.F., Zhang, X.Y., Yan, X.Y., 2017. Nitrate source apportionment using a combined dual isotope, chemical and bacterial property, and Bayesian model approach in river systems. J. Geophys. Res. - Biogeo. 122 (1), 2–14.
Xing, M., Liu, W., 2016. Using dual isotopes to identify sources and transformations of nitrogen in water catchments with different land uses, loess plateau of China. Environ. Sci. Pollut. Res. 23 (1), 388–401.
Xu, B.L., Shao, D.G., Tan, X.Z., Yang, X., Gu, W.Q., Li, H.X., 2017. Evaluation of soil water percolation under different irrigation practices, antecedent moisture and groundwater depths in paddy fields. Agric. Water Manag. 192, 149–158.
Xue, D., Botte, J., De Baets, B., Accoe, F., Nestler, A., Taylor, P., Boeckx, P., 2009. Present

limitations and future prospects of stable isotope methods for nitrate source identification in surface-and groundwater. Water Res. 43 (5), 1159–1170.
Yang, L., Han, J., Xue, J., Zeng, L., Shi, J., Wu, L., Jiang, Y., 2013. Nitrate source apportionment in a subtropical watershed using Bayesian model. Sci. Total Environ. 463, 340–347.
Yang, Y.Y., Toor, G.S., 2016. δ15N and δ18O reveal the sources of nitrate-nitrogen in urban residential stormwater runoff. Environ. Sci. Technol. 50 (6), 2881–2889.
Yi, Q., Chen, Q., Hu, L., Shi, W., 2017. Tracking nitrogen sources, transformation, and transport at a basin scale with complex plain river networks. Environ. Sci. Technol. 51 (10), 5396–5403.
Zhu, Q., Schmidt, J.P., Buda, A.R., Bryant, R.B., Folmar, G.J., 2011. Nitrogen loss from a mixed land use watershed as influenced by hydrology and seasons. J. Hydrol. 405 (3–4), 307–315.